

Microfluidic experimental platform for producing size-controlled three-dimensional spheroids

Hiroki Ota, Norihisa Miki*

Department of Mechanical Engineering, Keio University, 3-14-1 Hiyoshi, Kohoku-ku, Yokohama, Kanagawa 223-8522, Japan

ARTICLE INFO

Article history:

Available online 8 April 2011

Keywords:

Bio MEMS
Microfluidics
Microrotational flow
Spheroid

ABSTRACT

We propose a microfluidic experimental platform for producing size-controlled spheroids. Cells were aggregated into chambers arranged in an array by microrotational flow within 120 s to form spheroids. The cell density of the initial medium and hydrodynamic flow in the developed array could be adjusted while keeping the device geometry the same to control spheroid size with a standard deviation of less than 19% of the mean. Using this device, spheroids of HepG2 cells of various size categories could be maintained for three days in the chamber with medium exchange and could be continuously evaluated for topology and hepatic functions. Furthermore, CYP1A1 activities were found to increase with time to a constant level at three days. These results demonstrate that this device is readily applicable to producing and maintaining spheroids for *in vitro* drug screening and biological research.

© 2011 Elsevier B.V. All rights reserved.

1. Introduction

Cells live and function in the human body by interacting with neighboring cells and the extracellular matrix. Several cell types form spheroids, giving rise to functions not present in individual cells [1,2]. For example, aggregation of hepatocytes into spheroids results in the emergence of about 500 liver-specific functions, such as expressing new proteins and cell signaling. These spheroids appear to have tissue-like structures and a larger number of and more complex metabolic functions than are present in individual cells.

Numerous devices for producing three-dimensional culture models have been developed in the last two decades to bridge the gap between *in vitro* assays and animal models [3–5]. These devices reduce experimental error and the costs associated with drug screening. The development in recent years of microfluidic technology, which permits manipulation of cells on a micrometer scale, has been used in devices for forming spheroids. Spheroid formation devices employ micropatterned surfaces with a polyethylene glycol hydrogel [6] or extracellular matrix [7], a microcontainer to trap cells [8], and microfluidic hydrodynamics [9] or hydrodynamic force [10] to achieve cellular patterning of embryonic stem cells. Spheroid formation platforms used to measure physiologically active substances need to satisfy four requirements: (1) good controllability in the formation of spheroids; (2) allowance for

spheroid growth; (3) allowance for culturing of formed spheroids for an extended period of time (i.e., longer than one day) with morphological observations at any time; and (4) allowance for input of reagents to the system that dye or chemically stimulate cells.

We previously reported a hepatic spheroid-forming chamber that uses microrotational flow to control the size of spheroids [11]. Perfusion media containing hepatocytes were introduced into a microchamber in which microrotational flow was generated. Cells were collected at the center of the microchamber, where they aggregated and formed spheroids. Spheroids with diameters in the range 130–430 μm (with a standard deviation of about 15% of the mean) could be formed. The reported spheroid-forming chamber was superior to other microfluidic devices in that the spheroid size could be controlled by varying the cell density of the medium and without altering the device geometry. Further, the chamber provided space for spheroid growth in the center with hydrodynamic support. However, the device reported in the previous study had limitations [11]. Throughput was low due to having only one chamber. The perfusion system frequently became clogged with cells, which disrupted flow in the chamber and allowed spheroids to flow out of the chamber. Consequently, tests were limited in duration to one day.

In the present study, to increase the spheroid production rate, we designed an array consisting of five sets of chambers arranged in series; each set consists of three chambers connected in parallel. This arrangement enabled us to form a mean of 11 spheroids per trial with size control comparable to the previous device. Modification of the device enabled culturing of spheroids of a specified diameter over a longer duration, which produced higher yields.

* Corresponding author. Tel.: +81 45 566 1430; fax: +81 45 566 1495.
E-mail address: ota-mikilab@keio.to (N. Miki).

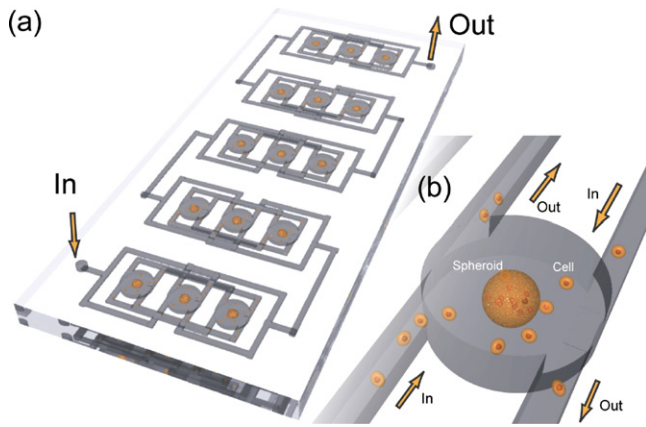


Fig. 1. (a) Schematic diagram of spheroid formation array. (b) Hepatocyte cell spheroids are produced by microrotational flow at the center of the chamber.

Using the modified device, we formed spheroids of HepG2 cells, and investigated the function of detoxification enzyme, cytochrome P450, by measuring ethoxyresorufin-O-deethylase (EROD) activity after three days of culturing. The results of this study demonstrate the potential of the developed array for biological research.

2. Experimental

2.1. Array design and fabrication

To increase spheroid production throughput, we designed an array of 15 microchambers arranged in 5 sets connected in parallel and 3 chambers coupled in series; each microchamber is a circular cylinder with two tangential inlet channels at the base and two outlet channels at the top (see Fig. 1). Microrotational flow is generated by the fluid flowing from the two inlet channels. Water pressure loss increases with increasing number of chambers connected in series. The water pressure loss in the inlet and outlet channels in the chamber [12] is given by

$$\Delta p = \lambda \frac{(h + W)L}{4hW} \left(\frac{\rho U^2}{2} \right),$$

where h is the height, W is the width, L is the length, U is the flow speed, and ρ is the density. λ is the friction coefficient of the rectangular channel and it is given by

$$\lambda = \frac{64}{Re} k_c,$$

where k_c is determined from the channel aspect ratio and Re is the Reynolds number.

In the channels, $k_c = 0.90$, $Re = 1.2 \times 10^3$, $h = 100 \mu\text{m}$, $W = 100 \mu\text{m}$, $L = 2.6 \text{ mm}$, and $U = 0.92 \text{ m/s}$, giving $\Delta p = 264 \text{ Pa}$. From the Hagen–Poiseuille equation, the pressure loss of the circular cylinder in the chamber is given by

$$\Delta p = \frac{32\mu LU}{D^2},$$

where D is the diameter, U is the flow speed, and μ is the viscosity. In the circular cylinder, $D = 3 \text{ mm}$, $L = 1 \text{ mm}$, and $U = 2.6 \text{ mm/s}$, giving $\Delta p = 7.3 \text{ Pa}$. Thus, the total water pressure loss in one chamber is 1063 Pa. Up to five sets of chambers could be coupled in series, as the high water pressure required for more than five chambers may cause fractures in the PDMS device.

In addition, we designed the geometry of the three chambers connected in parallel such that the differences in the water pressure loss are sufficiently small to allow spheroids to be formed and maintained in all chambers (Fig. 1). Water pressure loss occurs in

three areas of chambers connected in parallel: inlet channel tangential to the chamber cylinder, rectangular sections, and straight sections in a channel that transfers the medium to the chamber at the periphery of a set. Water pressure losses in the rectangular and straight sections occur only in chambers at the periphery of a set, and this may give rise to different flow velocities in chambers at the periphery and in the center of a set.

The array was made from polydimethylsiloxane (PDMS) (Silpot 184 W/C, Dow Corning Corp.) (Fig. 2a); it was formed by the following process. First, a negative photoresist SU-8 (SU-8 10, MicroChem Corp.) was patterned to produce circular cylinders and channels with array geometries on a clean glass slide by photolithography. We used two different geometries for the upper and middle layers (Fig. 2(a-1) and (a-2)). Liquid PDMS was poured into the mold and cured on a hotplate at 65°C for 6 h. The cured PDMS was then peeled from the mold. A punch was used to open the inlets and outlets in the upper layer and the inlets, chamber, and through-holes in the middle layer. The upper layer, middle layer, and bottom cover were aligned and bonded using an oxygen plasma treatment. In this study, spheroids with diameters of about $180 \mu\text{m}$ were targeted since cell necrosis occurs in the cores of spheroids with diameters greater than $180 \mu\text{m}$ [13,14]. We formed a SU-8 mold with a 3-mm-diameter chamber, which could form spheroids with diameters in the range $130\text{--}240 \mu\text{m}$ [11]. The channels connecting the chambers were $100 \mu\text{m}$ wide and $100 \mu\text{m}$ high (Fig. 2(b)).

3. Perfusion system set up

Since it takes at least one day to produce spheroids with enhanced functions [6], the device in the present study was designed to have a steady flow over a long duration. The following modifications were made to the perfusion system that employed a peristaltic pump, a reservoir, a dampener, and shredder channels for the production of HepG2 spheroids in our previous study [11]. In this system, the pump generates pulsatile flow by intermittently compressing the tube, and the dampener absorbs these pulsations by trapping air. Shredder channels consisting of 60 channels are used to prevent large cell aggregations from entering the inlet and outlet channels. These channels either break up such aggregations by shear stress or trap them.

To prevent cell aggregations from entering and becoming trapped in the channels as was observed in the previous system due to variation in velocity distributions after one day, we modified the reservoir and added a filtration system in parallel with the shredder channels to remove cells that had not been formed into spheroids (Fig. 3). This modified system maintained a constant rotational flow in the chamber enabling higher yields and allowed spheroids to be cultured for longer than in the previous system. A new filter system was designed to prevent clogging in shredder channels tangential to the chamber. Shredder channels in the previous model became clogged after one day due to the formation of cell aggregations in the tubes and reservoir causing unstable perfusion flow and giving rise to unstable microrotational flow. The components of this newly developed system are briefly described below.

3.1. Reservoir

We used a four-sided pyramid reservoir chamber rather than a cubic one to prevent the formation of undesired cell aggregations and to reduce chamber volume (Fig. 4). In addition, an outlet at the base of the reservoir prevents cells from residing too long in the reservoir, to prevent cells from aggregating and forming spheroids in the reservoir. Reagents that dye or chemically stimulate cells are supplied to the system from the reservoir.

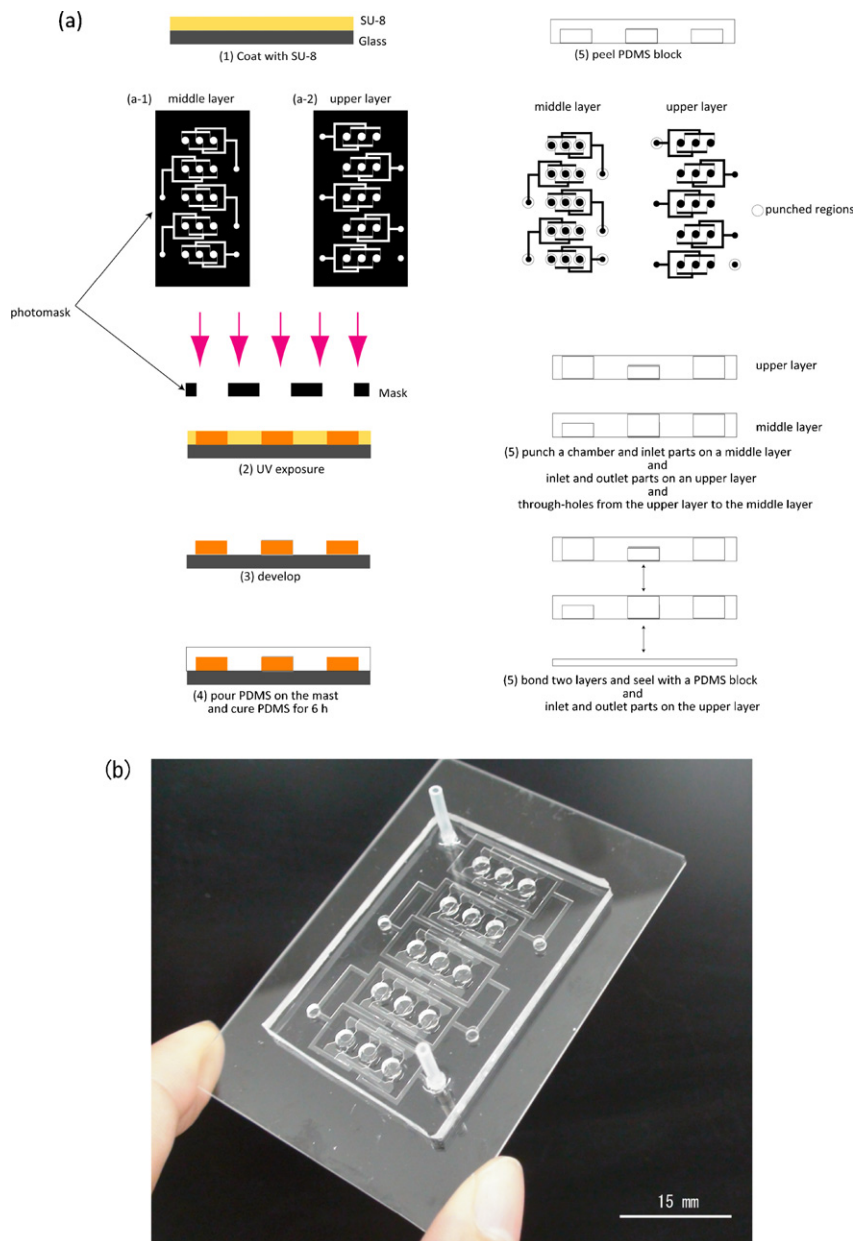


Fig. 2. Spheroid formation array. (a) Fabrication process. Array designs for (a-1) middle and (a-2) upper layers. (b) Photograph of fabricated device.

3.2. Filtration system

Cells often form undesired aggregations and clog channels in the chamber during long-term culture because excess cells that do not form spheroids continue to circulate in the system. Therefore, we developed a filtration system to remove excess cells from the media. Media are passed through a filtration system consisting of a peristaltic pump and a Terufusion® Final Filter PS (Terumo; pore size: 0.2 μm) to remove free cells, bacteria and debris, which sterilizes the media.

3.3. Filter

The newly designed filter (Fig. 5) consisted of four parts: Upper (Fig. 5a(A)) and lower (Fig. 5a(D)) polypropylene plates hold in place a filter (pore size, 30 μm ; track etched membrane, It4ip; Fig. 5a(B)) and a silicon sheet (Fig. 5a(C)). A channel 2 mm deep, 1 cm wide, and 2 cm long was made in the upper and lower plates,

and a well 8 mm deep, 1 cm wide, and 1 cm long was made in the lower plate. The silicon sheet was used to increase the adhesion between the upper and under plates, and together, this unit was used as the filter. In use, the medium containing cells flows through the channel in the under plate and cells and cell aggregations (>30 μm) are trapped on the filter or settle in the well in the under plate. The developed filter effectively traps small aggregations on the filter or in the well. However, small cell aggregations and cells were perfectly confined in the device, and then the cell density in the medium gradually decreased. Accordingly, after the spheroids had formed, we exchanged the filter for the shredder channels to prevent decreases in cell density.

4. Cell experiment

HepG2 cells were cultured in EMEM (DS Pharma Biomedical Co., Ltd.) and detached by EDTA and trypsin (DS Pharma Biomedical Co., Ltd.). To prevent cell aggregation, cells were subsequently cul-

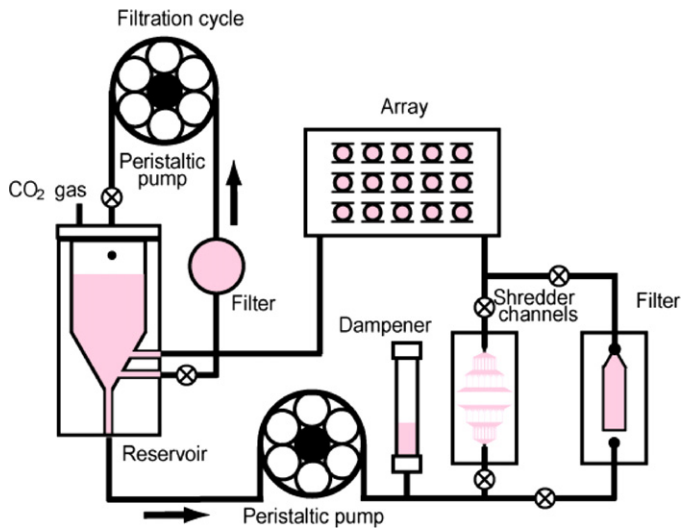


Fig. 3. Spheroid formation device consisting of an array and a perfusion system with a reservoir, shredder channels, a dampener, a filtration system, a peristaltic pump, and a filter.

tured for 30 min in a EMEM medium containing 1000 PU/ml dispase (Sanko Junyaku Co., Ltd.). Spheroid formation experiments were performed in an array using cell densities of 200×10^4 , 500×10^4 , and 1300×10^4 cells/ml. The temperature and pH of the medium circulating in the system were maintained by thermostatic bath and circulating CO₂ gas, respectively. First, the medium containing cells was introduced into the array at a volumetric flow rate of 3.3 ml/min until stable flow of the cells around the entire array was achieved. Second, the flow rate was gradually reduced to the flow

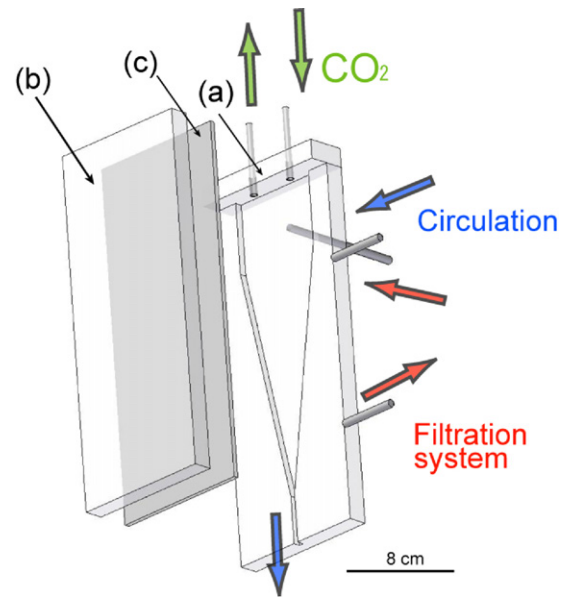


Fig. 4. Reservoir was assembled from three parts: (a) part with a chamber, (b) cover, and (c) silicon sheet. The silicon sheet was used to increase adhesion between the part with a chamber and the cover.

rate (approximately 1.2 ml/min) at which cells accumulate near the center of the chamber and form spheroids [11]. The closed region fluidically maintained the spheroids in the center of the chamber [11]. After spheroids formed, the filter pathway was used to prevent cell aggregations from entering the chamber (instead of closing the shredder channel pathway). To capture images of the spheroids,

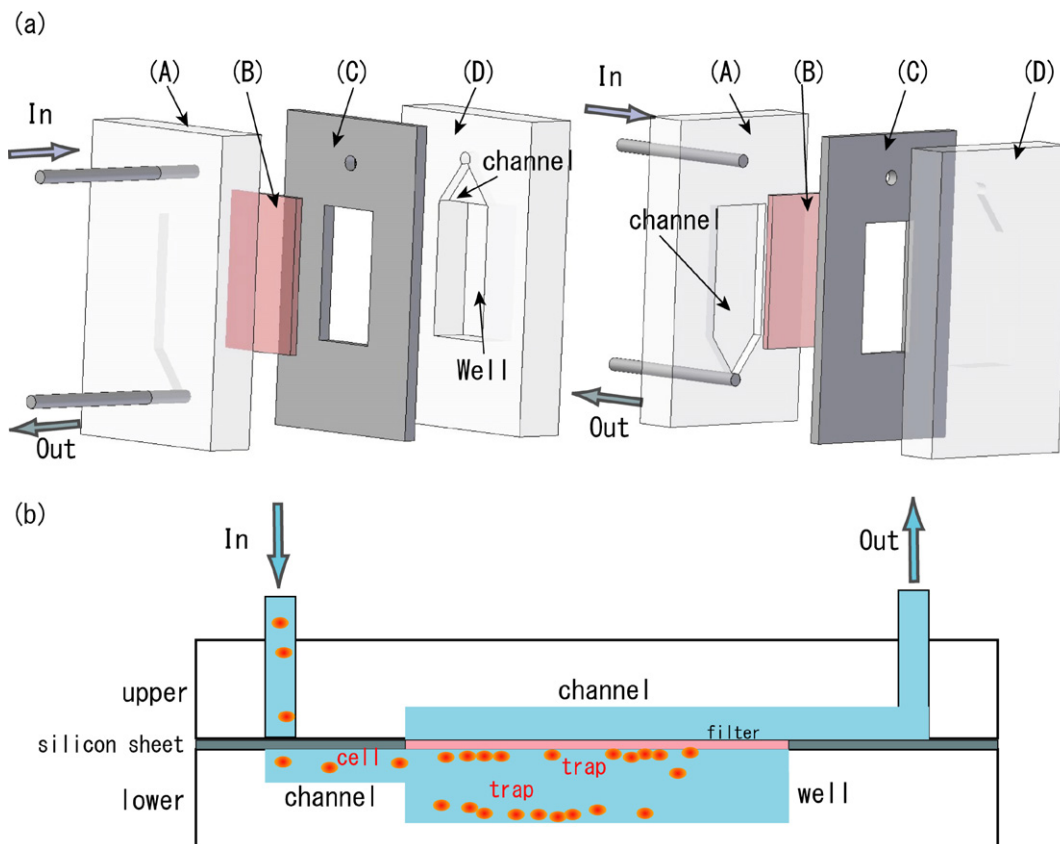


Fig. 5. (a) The filter consists of four parts: (A) an upper plate with a channel, (B) a filter, (C) a silicon sheet, and (D) a lower plate with a channel and a well. (b) Cross-sectional view of the filter. Small cell aggregations accumulate in the well or are trapped in the well and filter.

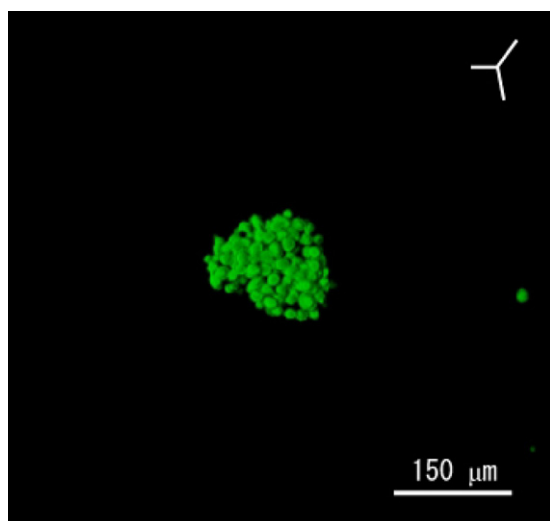


Fig. 6. Image of a spheroid stained with calcein AM.

a medium containing 4 μM calcein AM (Invitrogen) was added to the reservoir and spheroids were incubated for 20 min. Stationary two-dimensional fluorescence images were captured using a CCD camera (Cool SNAP-cf, Nippon Roper Co., Ltd. and EOS Kiss X3, Canon) and a confocal microscope (LSM7DUO, Carl Zeiss). The maximum and minimum diameters were measured using Image J.

5. Live/dead cell viability assay

Cells in the spheroids were incubated for 20 min in a medium containing 4 μM calcein acetoxymethyl ester (AM, Invitrogen) and 8 μM ethidium homodimer-1 (EthD-1, Invitrogen) to stain living cells. Two-dimensional fluorescence images were then captured using a CCD camera.

6. Cytochrome P450 activity

Cytochrome P450 activity was determined using the method of Behnia et al. [15]. Medium containing dicumarol (3,3'-methylenebis (4-hydroxycoumarin), Wako) and 3-methylcholanthrene (Sigma–Aldrich) was added starting one day before measurement. On the day of measurement, spheroids were incubated for 10 min in medium containing 20 μM resorufin ethyl ether (EROD, Sigma–Aldrich) and 80 μM dicumarol, the medium was exchanged twice with a fresh medium to remove residual dye, and fluorescences in images were measured to calculate the EROD activity. Based on the fluorescence images obtained using EROD, hepatic function activation could be determined [21].

7. Results and discussion

7.1. Spheroid size distribution in chamber and array

Microrotational flow was generated in the entire chamber at a volumetric flow rate of 3.3 ml/min. As the flow rate was reduced, the cells gradually aggregated and formed spheroids over about 120 s (Fig. 6). The spheroids had circular or elliptical profiles in two-dimensional images with random rotations (i.e., the rotational axis was constantly changing) at the center of the chamber, indicating that the spheroids are ellipsoidal or spherical.

Spheroids formed in a mean of 11 of the 15 chambers during five trials, and the spheroid formation throughput was 11 times higher than that for the single chamber device. Failure to produce spheroids was attributed to fabrication errors.

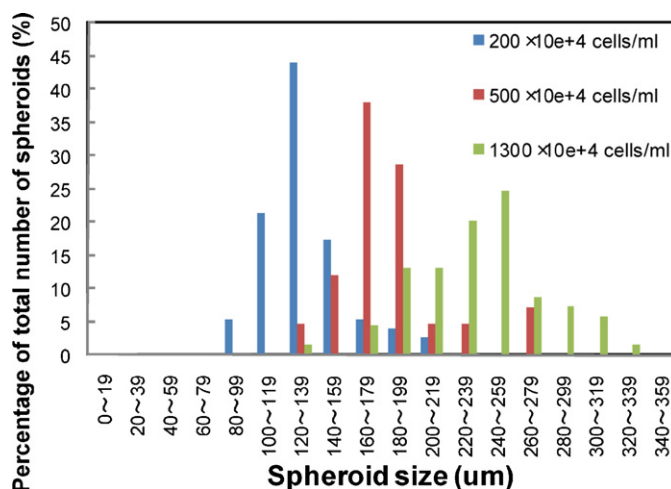


Fig. 7. Spheroid size distribution in array with different starting cell culture concentrations.

A volumetric flow rate of 1.2 ml/min was required to maintain stability and rotation of formed cell aggregations. The spheroid formation mechanism and the duration required to form spheroids were the same as in the single-chamber device. However, the volumetric flow rate required to generate microrotational flow and to ensure that the spheroids remain in the chamber was three times higher than that in a single-chamber device [11]. This is because three chambers are connected in parallel in each set. As the number of chambers connected in parallel in one set increases, the volumetric flow rate required to generate microrotation and to ensure that spheroids remain in the chamber increases.

The spheroids were nearly circular or ellipsoidal because cells adhered to each other in a random manner in rotation in the confined region [11]. In this study, we defined the spheroid diameter as the mean of the long and short axis lengths. Spheroids formed in an array with 3-mm-diameter chambers and starting cell densities of 200×10^4 , 500×10^4 , and 1300×10^4 cells/ml had mean (standard deviation) sizes of 134 ± 25 , 180 ± 30 , and 237 ± 40 μm , respectively, and the standard deviations represented 18.7%, 16.6%, and 16.9% of the mean, respectively (Fig. 7). Our previous study with a single-chamber device showed that the standard deviation was 15% of the mean for hepatic spheroids with diameters in the range 130–430 μm . The present results demonstrate that spheroid diameter is well controlled in an array with 15 chambers.

Curcio et al. reported size distributions for spheroids formed using a rotating-wall polystyrene system and a rotating-wall membrane system [14]. They were unable to create spheroids with diameters over 150 μm , even by varying the cell density in the medium. However, many spheroids with diameters less than 150 μm could be created in a single experiment, representing a high proportion (92.2%) of the total number of spheroids.

A culture array using a collagen/polyethylene glycol microcontact printing technique could create 200 spheroids on a single chip [16] and the spheroids on a Col/PEG SM chip had a uniform diameter distribution (155 ± 8 μm). A cell trapping microcontainer had a high throughput and high controllability of spheroid size by physically trapping cells. These devices can produce more spheroids in a single assay with more highly controlled spheroid size than in our system. However, our array uses only hydrodynamic forces to concentrate the medium in the center of the chamber and thus provides space for spheroids to grow.

In this study, we used HepG2 to verify the effectiveness of the array in forming spheroids. In the future, spheroid formations of primary cell cultures of various organ cells [17] and stem cells (e.g., embryo stem cells or induced pluripotent stem cells) will have

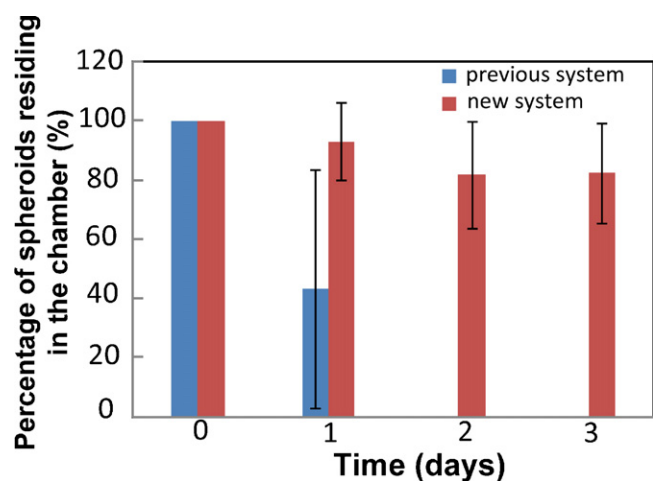


Fig. 8. Percentage of formed spheroids residing in the chamber for the previous and new systems for 0, 1, 2, and 3 days.

many applications in biological research and drug screening [9]. It will be important for spheroid formation chambers to have space for spheroid growth since spheroids formed from stem cells grow to large sizes [18].

7.2. Long-term culture of spheroids

Several days are required to enhance the connections between the constituent cells of spheroids through adhesion molecules such as integrin and cadherin and to improve the functions of spheroids [19]. Therefore, spheroid forming devices need to provide rotating spheroids with a steady flow of cell suspensions for several days and allow *in situ* monitoring of morphology and function. Fig. 8 shows a comparison of residence time in the chambers for the previous and new devices. No spheroids remained in the chamber of the previous device after two days because of the inability to maintain flow in the chamber. The system developed in the present study enabled more than 80% of the formed spheroids to gently rotate and be cultured in the chamber for three days (Fig. 8).

Fig. 9a shows an optical image and Fig. 9(b) and (c) shows fluorescent images of formed spheroids stained with calcein AM and EthD-1, respectively, after three days. Little fluorescence was observed from EthD-1 stained cells, but fluorescence was observed from calcein (compare Figs. 9(b) and (c)), indicating that the spheroids have a high cell viability after three days in the chamber.

Fig. 10 shows that the size of all spheroids remained constant over three days. The maximum relative change in the spheroid sizes over three days was 1.5% (see Fig. 10(d)). Liu et al. [20] demonstrate using WST-1 assay that the number of cells in a spheroid formed

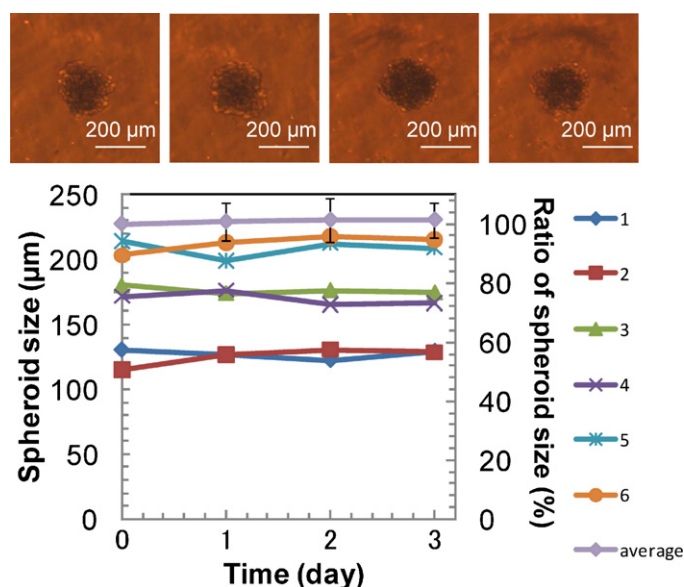


Fig. 10. Morphology of HepG2 aggregations at (a) 0, (b) 1 (c) 2, and (d) 3 days during spheroid formation. (d) Change in spheroid diameter. Legend on the right indicates number of spheroids. In the legend, “average” refers to mean ratio for all spheroid sizes normalized to the size at 0 h. Left axis represents sample size and right axis shows the ratio.

from HepG2 using a gyratory shaker remained constant over 21 days [20]. On the other hand, cell aggregations formed from HepG2 by a hanging-drop culture produced a compact spheroid after one day [19] and became smaller with time, shrinking rapidly over the first 12 h. As the hanging-drop culture involves culturing and aggregating cells in a drop of culture medium suspended from the lid of a culture dish, cells settle out and aggregate due to microgravity acting on each drop. Thus, a gravitational force directed toward the center of the chamber constantly acts on the cells, forcing the spheroids to shrink. In the chamber of this device, hydrodynamic forces (which are not directed toward the center of the chamber) confine a formed spheroid to the center of the chamber, and the sizes of spheroids did not vary over three days.

7.3. Time-dependent change in hepatic function of formed spheroids

Fig. 11 shows that the metabolic function (as indicated by CYP1A1 activity) of the formed spheroids increased over time. Hepatic function activation was assessed by analyzing fluorescence images obtained using EROD [21]. In this analysis, the change in the fluorescence intensity with time may depend on the spheroid size.

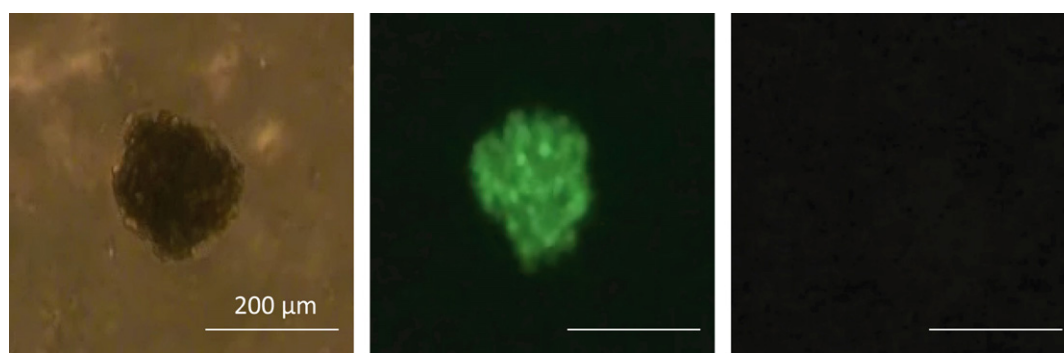


Fig. 9. Spheroid stained with calcein AM and EthD-1 after culturing for three days to determine cell viability. (a) Optical image and fluorescence images obtained using (b) calcein AM and (c) EthD-1.

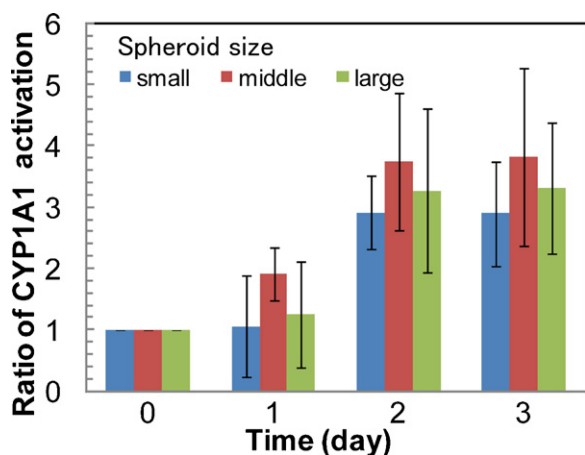


Fig. 11. CYP 1A1 activities of HepG2 at 0, 1, 2, and 3 days for small, medium, and large groups of spheroids with mean diameters in the ranges 110–140 μm , 160–180 μm , and 200–245 μm , respectively.

Hence, the spheroid sizes of the three groups at 0 h were measured and used to determine the control value percentages.

In humans, hepatocytes mainly activate the detoxification enzyme CYP1A1 and partially activate detoxification enzymes CYP1B1, CYP2C9, and CYP3A4 [22,23]. HepG2, which retains various hepatic functions, has a low CYP activity. However, Wilkening et al. verified by reverse transcriptase polymerase chain reaction (RT-PCR) that HepG2 has high CYP1A1 and CYP3A7 activities [24]. Furthermore, expression of CYP1A1 in HepG2 was directly demonstrated by GFP [25]. Therefore, we chose to use the EROD method, which can be used to measure CYP1A1 activation, to verify activation of detoxification enzymes.

The EROD activity of spheroids formed by our array increased after one day and became constant after two days (see Fig. 11). As mentioned above, it is possible that fluorescence intensity depends on spheroid size. However, Fig. 11 shows that the sizes of all three types of spheroids remained constant over three days. Consequently, it is not necessary to consider size effects. In addition, in the light of Westerink's study [20], it is high unlikely that the number of cells in a spheroid increases by a factor of three or four without a change in the spheroid size. Thus, it is reasonable to assume that the detoxification activity of the spheroids increases with time and becomes saturated after two days.

We identified spheroids based on their sizes and performed EROD assays. Spheroids in small, medium, and large groups had diameters in the ranges 110–140 μm , 160–180 μm , and 200–245 μm , respectively. Tamura et al. demonstrated that the albumin secretion activity per cell remains almost constant in spheroids with diameters in the range 133–267 μm over three days [16]. Our CYP1A1 results corroborate their results. The presence of necrotic cells in spheroids is undesirable for drug screening and biological research. Therefore, spheroids with diameters less than 180 μm are suitable for drug screening and biological research since their function increases over two days.

8. Conclusion

In this study, we demonstrated the effectiveness of our newly developed array for forming and measuring three-dimensional spheroids of various sizes. An array consisting of 15 chambers produced a mean of 11 spheroids per trial, and spheroid diameter was controlled in the range 130–237 μm . The standard deviations of the spheroids produced from initial cell densities of 200×10^4 , 500×10^4 , and 1300×10^4 cells/ml were 18.7%, 16.6%, and 16.9% of

the means, respectively. Therefore, the standard deviation of the spheroid size was less than 19% of the mean.

The developed device, which consists of an array, a reservoir, a dampener, shredder channels, a filtration system, a filter, and a peristaltic pump, enabled observation of spheroids and measurement of the hepatic functions for periods of over three days. Experiments performed with the device indicated that the sizes of the formed spheroids remain constant and that their CYP1A1 activities increase over time.

Acknowledgements

This work was supported in part by a Grant-in-Aid for Scientific Research (S) (21226006) from the Ministry of Education, Culture, Sports, Science and Technology (MEXT) and the Scientific Research of Priority Areas, System Cell Engineering by Multi-scale Manipulation. It was also supported in part by Keio University through the Keio Gijuku Fukuzawa Memorial Fund for the Advancement of Education and Research.

References

- [1] A.P. de Barros, C.M. Takiya, L.R. Garzoni, M.L. Leal-Ferreira, H.S. Dutra, L.B. Chiarini, M.N. Meirelles, R. Borojevic, M.I. Rossi, Osteoblasts and bone marrow mesenchymal stromal cells control hematopoietic stem cell migration and proliferation in 3D in vitro model, *PLoS One* 5 (2010) e9093.
- [2] J. Op Den Buijs, E.L. Ritman, D. Dragomir-Daescu, Validation of a fluid–structure interaction model of solute transport in pores of cyclically deformed tissue scaffolds, *Tissue Eng. C: Methods* (2010) (Epub ahead of print).
- [3] S.L. Nyberg, E.S. Baskin-Bey, W. Kremers, M. Prieto, M.L. Henry, M.D. Stegall, Improving the prediction of donor kidney quality: deceased donor score and resistive indices, *Liver Transpl.* 11 (2005) 901–910.
- [4] M. Wartenberg, F. Dönmez, F.C. Ling, H. Acker, J. Hescheler, H. Sauer, Tumor-induced angiogenesis studied in confrontation cultures of multicellular tumor spheroids and embryoid bodies grown from pluripotent embryonic stem cells, *FASEB J.* 15 (2001) 995–1005.
- [5] M. Ingram, G.B. Techy, R. Saroufeem, O. Yazan, K.S. Narayan, T.J. Goodwin, G.F. Spaulding, Three-dimensional growth patterns of various human tumor cell lines in simulated microgravity of a NASA bioreactor, *In Vitro Cell Dev. Biol. Anim.* 33 (1997) 459–466.
- [6] H. Otsuka, A. Hirano, Y. Nagasaki, T. Okano, Y. Horiike, K. Kataoka, Two-dimensional multiarray formation of hepatocyte spheroids on a microfabricated PEG-brush surface, *Chem. BioChem.* 5 (2004) 850–855.
- [7] S.R. Khetani, S.N. Bhatia, Microscale culture of human liver cells for drug development, *Nat. Biotechnol.* 26 (2008) 120–126.
- [8] E. Eschbach, S.S. Chatterjee, M. Noldner, E. Gottwald, H. Dertinger, K.F. Weibezahn, G. Knedlitschek, Microstructured scaffolds for liver tissue cultures of high cell density: morphological and biochemical characterization of tissue aggregates, *J. Cell Biochem.* 95 (2000) 243–255.
- [9] Y.S. Torisawa, B.H. Chueh, D. Huh, P. Ramamurthy, T.M. Roth, K.F. Barald, S. Takayama, Efficient formation of uniform-sized embryoid bodies using a compartmentalized microchannel device, *Lab Chip* 7 (2007) 770–776.
- [10] L.Y. Wu, D. Di Carlo, L.P. Lee, Microfluidic self-assembly of tumor spheroids for anticancer drug discovery, *Biomed. Microdevices* 10 (2008) 197–202.
- [11] H. Ota, R. Yamamoto, K. Deguchi, Y. Tanaka, Y. Kazoe, Y. Sato, N. Miki, Three-dimensional spheroid-forming lab-on-a-chip using micro-rotational flow, *Sens. Actuators B* 147 (2010) 359–365.
- [12] U. Cavallaro, G. Christofori, Cell adhesion and signalling by cadherins and Ig-CAMs in cancer, *Nat. Rev. Cancer* 4 (2004) 118–132.
- [13] J. Alvarez-Perez, P. Ballesteros, S. Cerdan, Microscopic images of intraspheroidal pH by 1 H magnetic resonance chemical shift imaging of pH sensitive indicators, *MAGMA* 18 (2005) 293–301.
- [14] E. Curcio, S. Salerno, G. Barbieri, L. De Bartolo, E. Drioli, A. Bader, Mass transfer and metabolic reactions in hepatocyte spheroids cultured in rotating wall gas-permeable membrane system, *Biomaterials* 28 (2007) 5487–5497.
- [15] K. Behnia, S. Bhatia, N. Jastromb, U. Balis, S. Sullivan, M. Yarmush, M. Toner, Xenobiotic metabolism by cultured primary porcine hepatocytes, *Tissue Eng.* 6 (2000) 467–479.
- [16] T. Tamura, Y. Sakai, K. Nakazawa, Two-dimensional microarray of HepG2 spheroids using collagen/polyethylene glycol micropatterned chip, *J. Mater. Sci. Mater. Med.* 19 (2008) 2071–2077.
- [17] A.P. Napolitano, D.M. Dean, A.J. Man, J. Youssef, D.N. Ho, A.P. Rago, M.P. Lech, J.R. Morgan, Scaffold-free three-dimensional cell culture utilizing micromolded nonadhesive hydrogels, *Biotechniques* 43 (2007) 496–500.

- [18] Y.S. Torisawa, B. Mosadegh, G.D. Luker, M. Morell, K.S. O'Shea, S. Takayama, Microfluidic hydrodynamic cellular patterning for systematic formation of co-culture spheroids, *Integr. Biol. (Camb.)* 1 (2009) 649–654.
- [19] R.Z. Lin, L.F. Chou, C.C. Chien, H.Y. Chang, Dynamic analysis of hepatoma spheroid formation: roles of E-cadherin and beta1-integrin, *Cell Tissue Res.* 324 (2006) 411–422.
- [20] J. Liu, L.A. Kuznetsova, G.O. Edwards, J. Xu, M. Ma, W.M. Purcell, S.K. Jackson, W.T. Coakley, Functional three-dimensional HepG2 aggregate cultures generated from an ultrasound trap: comparison with HepG2 spheroids, *J. Cell Biochem.* 102 (2007) 1180–1189.
- [21] T. Matsushita, K. Nakano, Y. Nishikura, K. Higuchi, A. Kiyota, R. Ueoka, Spheroid formation and functional restoration of human fetal hepatocytes on poly-amino acid-coated dishes after serial proliferation, *Cytotechnology* 42 (2003) 57–66.
- [22] J.C. Gautier, S. Lecoq, J. Cosme, A. Perret, P. Urban, P. Beaune, D. Pompon, Contribution of human cytochrome P450 to benzo[a]pyrene and benzo[a]pyrene-7,8-dihydrodiol metabolism, as predicted from heterologous expression in yeast, *Pharmacogenetics* 6 (1996) 489–499.
- [23] P. Sims, P.L. Grover, A. Swaisland, K. Pal, A. Hower, Metabolic activation of benzo(a)pyrene proceeds by a diol-epoxide, *Nature* 22 (1974) 326–328.
- [24] S. Wilkening, F. Stahl, A. Bader, Comparison of primary human hepatocytes and hepatoma cell line HepG2 with regard to their biotransformation properties, *Drug Metab. Dispos.* 31 (2003) 1035–1042.
- [25] T.N. Operaña, N. Nguyen, S. Chen, D. Beaton, R.H. Tukey, Human CYP1A1GFP expression in transgenic mice serves as a biomarker for environmental toxicant exposure, *Toxicol. Sci.* 95 (2007) 98–107.

Biographies

Hiroki Ota received his BE and ME degrees in applied physics from Keio University in 2005 and 2007, respectively, where he investigated the effect of endothelial permeability on photochemical reactions. Since 2008, he has been a PhD student at Keio University. He was supported by a research fellowship from Japan Society for the Promotion of Science (JSPS) from 2009 to 2011. His principal fields of interest include MEMS-based medical devices, microTAS, and tissue engineering.

Norihisa Miki received his BE, ME and PhD degrees in mechanical engineering from the University of Tokyo in 1996, 1998 and 2001, respectively. From 2001 to 2004 he was a postdoctoral associate and then a research engineer in the Department of Aeronautics and Astronautics at the Massachusetts Institute of Technology, where he worked on the development of a button-size silicon microgas turbine engine. In 2004 he joined the Department of Mechanical Engineering at Keio University, Kanagawa, Japan, as an assistant professor. He was a part-time researcher of Nano Photo Bio Group at Kanagawa Academy of Science (KAST) from 2006 to 2009 and is currently a researcher at Life BEANS (Bio Electromechanical Autonomous Nano Systems) Center, BEANS Laboratory (2007–), a part-time researcher in Bio Microsystems Project, KAST (2010–), and a member of PRESTO (Precursory Research for Embryonic Science and Technology), Japan Science and Technology Agency (JST) in the area of Information Environment and Humans (2010–). His principal fields of interests include MEMS-based human interface, nano- microfabrication technology, micro-TAS, bio and chemical sensors, and power MEMS. Prof. Miki is a vice chairperson of Professional Committee of Micro-Nano Science and Engineering in Japan Society of Mechanical Engineers (JSME) and a member of IEEE.